A Numerical Study of the Effect of Channel Insulator Discontinuity on Hall Thruster Discharge*†

Summer Locke and Uri Shumlak
Department of Aeronautics and Astronautics
University of Washington
BOX 352250
Seattle, WA 98195-2400
206-616-1986
locke@aa.washington.edu
shumlak@aa.washington.edu

J.M. Fife
Electric Propulsion Group
Air Force Research Laboratory
AFRL/PRRS
1 Ara Road
Edwards AFB, CA 93524-7190
805-275-6792
John.Fife@edwards.af.mil

IEPC-01-23

We present results from a numerical investigation of using a section of channel insulator with lower secondary electron emission coefficient to increase thrust and efficiency or reduce insulator erosion in an SPT-type Hall thruster. An evolved 2-D hybrid particle-in-cell numerical Hall thruster model, HPHall, was used. Various cases were run to compare the effect of location and width of the inserted insulator section on the plasma response. An SPT-70 geometry with channel insulator material similar to BN was used as a baseline configuration with sections of BNAlN ceramic. We found that a 6% reduction in total ion flux to the walls with a 3.7% reduction in the maximum ion flux to the walls near the thruster exit could be obtained. We also found that thrust and efficiency could be increased by 7% and 6% at the expense of a 30% increase in ion flux to the walls. We have shown that we might be able to modify the local plasma properties with this passive technique and it should be investigated experimentally.

Introduction

This paper presents comparisons of results from an evolved 2-D numerical Hall thruster simulation, HPHall, to investigate replacing a section of channel insulator with a different ceramic to increase thruster performance or reduce channel wall erosion near the exit. A section of ceramic material with lower secondary electron emission (SEE) coefficient is used in attempt to localize the electric field. This study was inspired by the idea, originally proposed by Fructman and Fisch, of using a localized electric field to control the location and extent of the ion acceleration layer [2]. Subsequent experiments by Raitses et. al. used segmented electrodes to localize the voltage drop instead of SEE coefficient. An approximate 10% to 20% reduction in plume divergence angle at the expense of efficiency was reported in these experiments [3, 4]. If replacing a section of insulator material has a similar effect, it also has the advantage of being a passive control.

In our initial studies of the effect of changing the SEE coefficient of the entire channel insulator on the thruster performance characteristics [5], we found that decreasing the SEE coefficient led to increased thrust and efficiency. We then used a simplified 1-D model

* Presented as Paper IEPC-01-23 at the 27th International Electric Propulsion Conference, Pasadena, CA, 15-19 October, 2001.

to conduct a preliminary study of the effect of a single discontinuity on the thruster discharge properties [1]. From the 1-D results we found that a single SEE coefficient discontinuity placed between the anode and the sonic transition point did not significantly affect the potential drop or electron temperature. Here we use an evolved 2-D hybrid-PIC model, HPHall, to investigate the effect that the location and width of a section of insulator material with a lower SEE coefficient has on the thruster discharge and performance characteristics.

Numerical Model

HPHall is a transient 2-D simulation operating in cylindrical coordinates. Comparisons of HPHall to experimental results for the SPT-70 Hall thruster [5] have shown that HPHall can model the thruster efficiency and thrust to within 5%.

Governing Equations

The following is a brief description of the theory and governing equations used in HPHall. This description summarizes previous publications [5, 6].

Electron Equations

The simplified electron equations consist of a generalized Ohm's law, a current conservation equation, and an electron energy equation. A Maxwellian electron distribution, quasineutrality, and a particular ion field are assumed. The electron energy equation is reduced to quasi-one-dimensional form by assuming that the electron temperature does not vary along magnetic field lines. The generalized Ohm's Law is used for electron diffusion across magnetic field lines and the cross-field electron velocity is computed using classical and Bohm mobility. The Bohm mobility factor was set to 0.15 for this investigation, which has previously been found to be the "best-fit" to experimental data [5].

Heavy Species

Current conservation, the bulk ionization rate, and the equations of motion for the ions and neutrals complete the model for the heavy species. Ions and neutrals are tracked using a particle-in-cell method and the ion and electron systems are linked by charge neutrality. The bulk electron-neutral ionization rate is determined by integrating the Drawin [7] cross-section over a Maxwellian electron distribution.

Wall Effects

The interaction of Hall thruster plasma with the insulator wall is a function of the secondary electron emission coefficient of the insulator material. Experimental data show that the ratio of secondary to primary electrons, δ, can be described using Vaughan's general formula for SEE yield [8] in the low energy regime where it reduces to a power law.

$$\delta = \left(\frac{T_e}{T_{e,BP}} \right)^{\alpha} \tag{1}$$

The wall model in HPHall allows for a negative wall potential with an ion-attracting near-wall sheath, and a positive wall potential with an ion-repelling near-wall sheath. The electron temperature where the wall potential reverses is termed the breakpoint temperature, $T_{e,BP}$. Recent results from HPHall show that when T_e approaches $T_{e,BP}$, the heat loss grows so large that it is effectively limited to $T_{e,BP}$. The equation for energy lost to the wall was derived from integrating the primary and secondary electron energy fluxes across Maxwellian distributions. The near-wall electron conductivity, I_w, is determined by calculating the downstream distance traveled by the guiding center of low-energy secondary electrons starting at rest at the wall in crossed electric and magnetic fields.

$$I_w = \Gamma_{\text{sec}} \left(\frac{2\pi r E m_e}{B^2 \sin(\theta)} \right) \tag{2}$$

In equation 2, θ is the angle of incidence of the magnetic field line with the wall and Γ_{sec} is the secondary electron flux from the channel wall.

Boundary Conditions

Electron temperature is directly fixed at the cathode and a zero slope condition is imposed on electron temperature at the anode. Although HPHall is capable of modeling the background chamber pressure, it was set to zero for this study. Propellant feed particles are placed randomly within the injector region and have random trajectories that correspond to a half-range Maxwellian distribution at a temperature of 1000 K.

Numerical Method

The magnetic field is generated as a pre-process, which solves Laplace's equation on regions exterior to infinitely permeable iron poles. The governing equations are solved time accurately by separating the slow time scale (ion and neutral) motion from the fast time scale (electron) motion and iterating successively. Individual ion and neutral atoms are simulated using a PIC method. The electron motion is solved using a modified Forward Time Centered Space (FTCS) method. Numerical stability and spatial discretization for the SPT-70 geometry used here were verified by successive reduction of the time step and cell size. Solutions from this time-accurate simulation are assumed to have reached steady state when the amplitude remains roughly the same over five long-period oscillations.

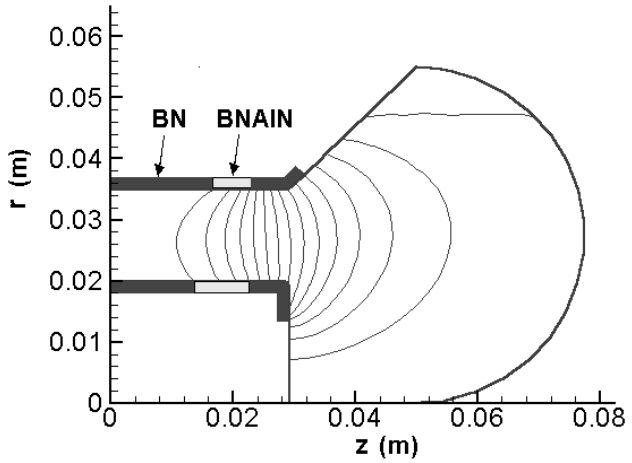

Figure 1: A 2-D map of the computational domain showing the thruster channel ($z \leq 0.029$ m), the exit region and the applied magnetic field lines. Also an illustration of how a section of BNAlN insulator is inserted within a BN channel such that it is bounded by the same lines of constant magnetic field.

Approach

HPHall was modified to allow two discontinuities in SEE coefficient of the channel insulator. The discontinuities are implemented in 1-D along lines of constant magnetic field (constant λ lines). Figure 1 illustrates how these lines map to two dimensions. In figure 1, z is the axial coordinate and r is the radial coordinate. We inserted sections of material with lower SEE coefficient at various locations between the anode and cathode. This insulator section insert is not symmetric about the radial center of the channel, but is bounded by the same magnetic field lines, as shown in figure 1.

The geometry modeled was similar to that of an SPT-70, with a channel length of 29 mm, and a channel width of 15 mm. The cathode is located at 34.2 mm from the anode and channel insulator material extends to the cathode. Propellant flow rate is 2.34 mg/s xenon, and discharge voltage is 300V. As a baseline, the entire channel insulator has properties similar to boron nitride (BN), whose secondary electron emission coefficient properties are provided in Table 1 and illustrated in Figure 2.

Table 1. Coefficients and Exponents of SEE Yield

Material	$T_{e,BP}$ (breakpoint)	α (exponent)
BN	16.65 eV	0.576
Baseline Case	16 eV	0.576
BNAlN[9]	70.2 eV	0.53

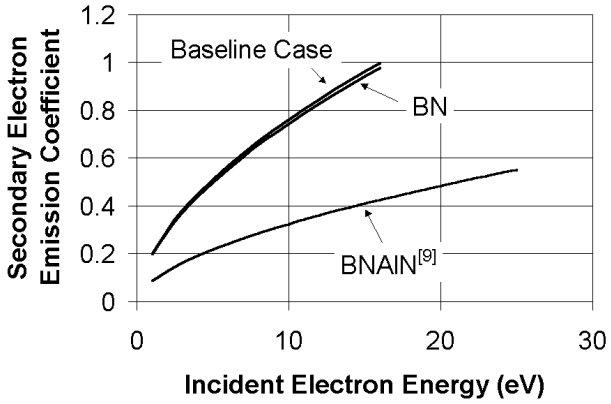

Figure 2: Secondary Electron Emission Coefficient as a Function of Incident Electron Energy for the Insulator Materials Used in This Study.

As a numerical experiment, we inserted single 2-mm, 4-mm and 6-mm sections of boron nitride aluminum nitride (BNAlN) ceramic in various locations within the channel insulator between the anode and cathode, while the rest is BN. All case studies were run for 10,000 iterations and reached a quasi-steady state. The following results are averaged over the 10,000 iterations.

Results and Discussion

We assessed the effects of location and width of different insulator sections on the thruster performance characteristics. The time-averaged thrust, efficiency, and total ion wall current to discharge current fraction are compared for various cases in figures 3, 4 and 5, respectively. Note that the thrust was computed as the time rate of axial ion momentum leaving the boundaries of the computational domain. These results show that two separate operating regimes can be obtained by varying the location of the inserted insulator section. A regime with increased thrust and efficiency is obtained when a majority of the section with lower SEE coefficient is placed forward (toward the cathode) of the sonic transition. In this regime, the thrust and efficiency continue to increase as the section width increases and are accompanied by an increase in ion current lost to the walls. This suggests that the channel wall configuration could be optimized for thrust and efficiency based on an acceptable level of increased channel wall erosion. The other regime with decreased ion loss to the walls is obtained when a majority of the section with lower SEE coefficient is placed behind (toward the anode from) the sonic transition. In this regime, the total ion loss to the walls can be reduced while maintaining or slightly increasing the thrust and efficiency. This suggests that the channel wall erosion could be reduced without adversely affecting the thruster performance characteristics. To compare these numerical results to existing experimental results, the total ion current to the wall is 0.22 Amps for the baseline case. Bishaev and Kim [10] experimentally estimated that the ion loss to the walls is 1.0 Amp for SPT-100 class thrusters. Scaling this value based on area would predict a 0.5 Amp total wall current for SPT-70 class thrusters [6]. This indicates that HPHall may be under-predicting the ion wall current for the baseline case and all other cases, however, for this study we are primarily interested in relative effects.

To gain and understanding of the effects that drive the observed improvements, the axial profiles of some parameters of interest for case 1 and case 2 (marked on figures 3 through 5) are compared with the baseline case in figures 6 through 13. Both case 1 and case 2 use a 6-mm wide section of BNAlN within an insulator material similar to BN (table 1, figure 2). The baseline case is a continuous insulator of the

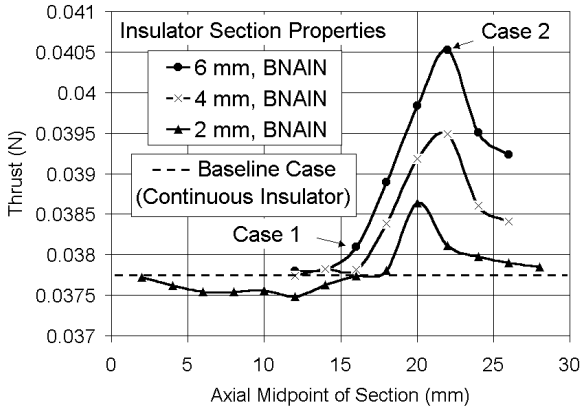

Figure 3: Variation in time-averaged thrust as the location and width of an inserted section of BNAlN is varied along the channel.

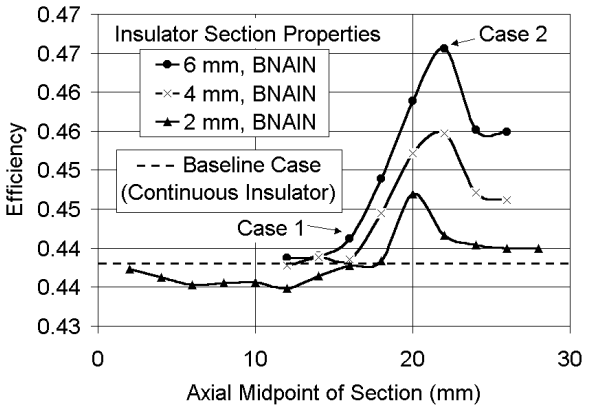

Figure 4: Variation in time-averaged efficiency as the location and width of an inserted section of BNAlN is varied along the channel.

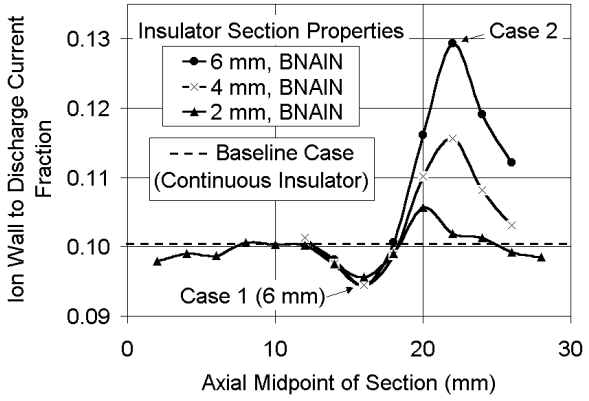

Figure 5: Variation in time-averaged ion wall to discharge current fraction as the location and width of an inserted section of BNAlN is varied along the channel.

material similar to BN. Since the parameters shown in these figures were computed with respect to constant magnetic field lines, the axial coordinate, z_{mean}, in these figures is the mean value of the spatial coordinate, z, along a particular constant magnetic field line. The first parameter of interest is the axial profile of SEE coefficient for these cases, shown in figure 6. This illustrates how the inserted insulator section affects the SEE coefficient when placed in different regions of the thruster. Since this is the control parameter for this study, it is a key reference for the following discussion.

In the increased efficiency and thrust regime, the total efficiency increase is driven by the increased propellant utilization efficiency resulting from increased electron temperature. Case 2 is in this regime and has a thrust increase of 7% and an efficiency increase of 6% over the baseline case. The increased electron temperature for case 2 (figure 7) results in a higher ionization rate (figure 8), plasma density (figure 9) and an extended ionization zone. This is supported by data from a previous HPHall study where an increase in propellant utilization efficiency with maximum electron temperature was also observed when the SEE coefficient of the entire insulator was varied [5]. Comparing case 1 and case 2 in figures 6 and 7, we can see that a much more dramatic electron temperature increase occurs when the section with lower SEE coefficient is placed forward of the ionization layer. This is due to the dominance of ionization losses over wall losses in the ionization region and was also seen in our previous 1-D and parametric studies [1]. Thus, the increased thrust and efficiency regime is obtained when the SEE coefficient is reduced in the region forward (toward the cathode) of the ionization layer, where the reduced wall losses can significantly increase the electron temperature.

The increased thrust and efficiency regime is accompanied by an increase in ion flux to the walls (figure 5). In case 2, the total ion wall current to discharge current fraction increased by 30% over the baseline case. This is primarily a result of two effects. The extended ionization layer in case 2 pushes the sonic transition and the acceleration layer closer to the cathode (figure 11), into the region of defocusing magnetic field lines (figure 1). Also, the localized electric field in the region of the inserted section

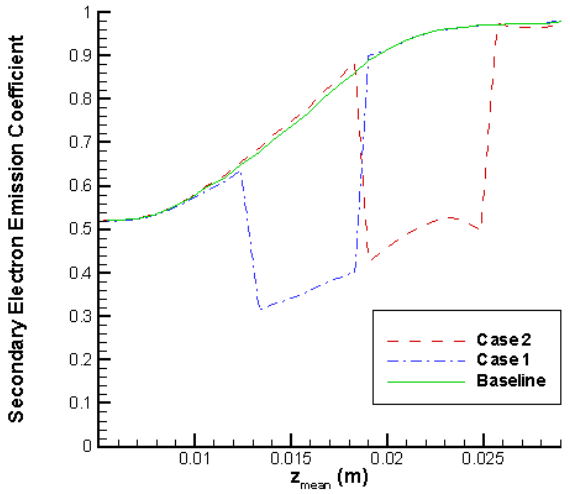

Figure 6: Time-Averaged Axial Profile of Secondary Electron Emission (SEE) Coefficient. The baseline case represents a continuous insulator material similar to BN. In case 1 and case 2, part of the insulator is replaced by a 6-mm wide section of BNAlN, which has a lower SEE coefficient. These cases correspond to those marked on figures 3 through 5.

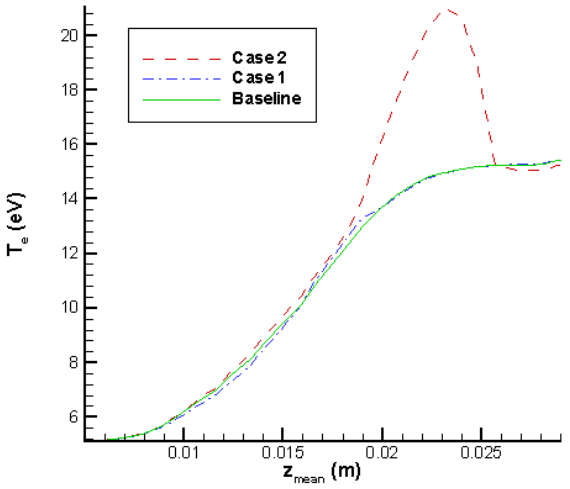

Figure 7: Time-Averaged Axial Profile of Electron Temperature. The temperature increase for case 2 is due to the reduced SEE coefficient of the inserted insulator section in that region. The effect of the inserted insulator section on the electron temperature for case 1 is less significant than for case 2. These cases correspond to those marked on figures 3 through 5.

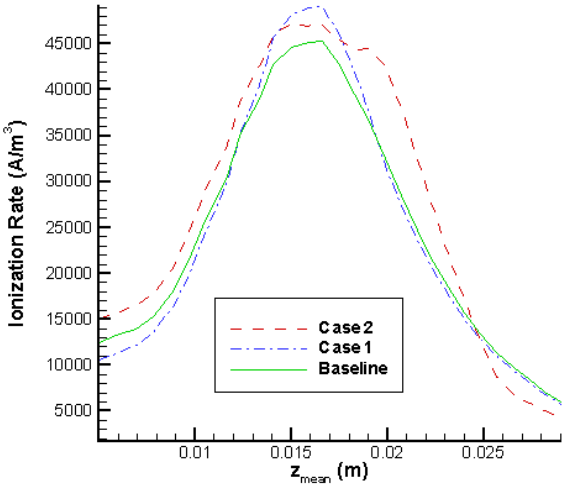

Figure 8: Time-Averaged Axial Profile of Ionization Rate. Both case 1 and case 2 have a higher ionization rate than the baseline case, resulting in a higher propellant utilization efficiency. Also, case 2 has an extended ionization layer. These cases correspond to those marked on figures 3 through 5.

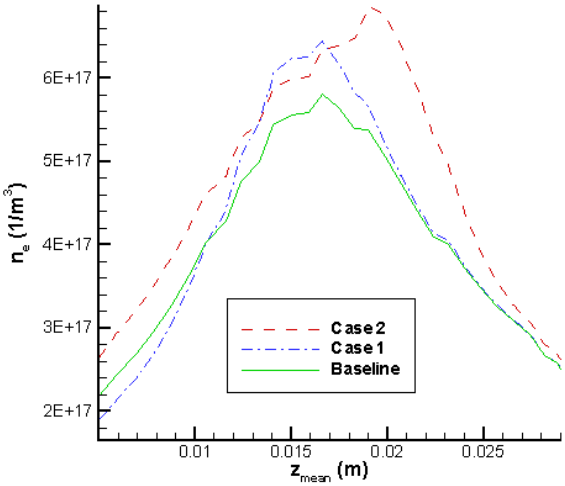

Figure 9: Time-Averaged Axial Profile of Plasma Density. This data is included for reference. These cases correspond to those marked on figures 3 through 5.

(figure 13) causes the acceleration layer to be more localized in the region of defocusing magnetic field lines within the thruster. Note that the inserted section is more effective at modifying the electric field and potential drop (figure 12) when it is placed forward of the ionization layer. This was also suggested by our previous 1-D and parametric studies [1]. These two effects cause more ions to be directed toward the chamber walls near the thruster exit, which could result in increased channel wall erosion.

Case 1 is in the regime with decreased ion loss to the walls. A comparison of case 1 with the baseline case shows that a 6% reduction in the total ion wall current to discharge current fraction is accompanied by a thrust and efficiency increase of approximately 1% (figures 3 through 5). This regime is believed to result from the localization of the electric field in the region of focusing magnetic field lines where the insulator section with lower SEE coefficient is located (figures 1, 6 and 13). The localized electric field causes more of the ion acceleration to occur in this region, thus the ion flow is more focused downstream. This is supported by the observation that the ion flux to the walls is reduced in the region downstream (toward the cathode) of the localized electric field (figures 10 and 13). The maximum ion flux to the walls near the thruster exit was reduced by 3.7% in case 1. The effectiveness of the insulator section for localizing the electric field in the region of focusing magnetic field lines is limited due to the dominance of ionization losses over wall losses. This could limit the effectiveness of using reduced SEE coefficient to reduce wall erosion.

The results of this study indicate that a section of insulator material with lower SEE coefficient might be effective for either reducing insulator erosion without adversely affecting the thruster efficiency and thrust or increasing efficiency and thrust with an increase in ion flux to the walls. The effectiveness of using this technique to modify the ion flux to the walls appears to strongly depend on the applied magnetic field configuration. Based on these results, we recommend that this passive technique be investigated experimentally. For this, additional results from HPHall should be studied to further optimize the channel insulator configuration. Possible additional improvements for the high performance regime could be to use a sputter resistant insulator material near the thruster exit or a focusing magnetic field in the region of the inserted section. It would also be important to quantify the effect of the insulator discontinuities on the oscillatory characteristics of the discharge in future studies.

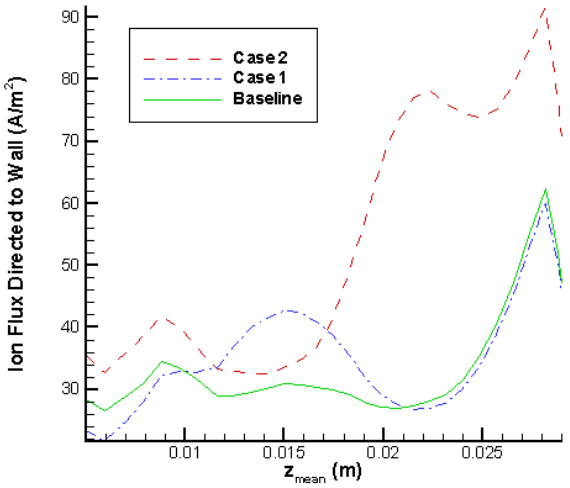

Figure 10: Time-Averaged Axial Profile of Ion Flux to the Channel Walls. Case 1 has decreased ion flux to the walls near the thruster exit (at z_{mean} = 29 mm) compared to the baseline case. The flux is increased throughout the channel for case 2. These cases correspond to those marked on figures 3 through 5.

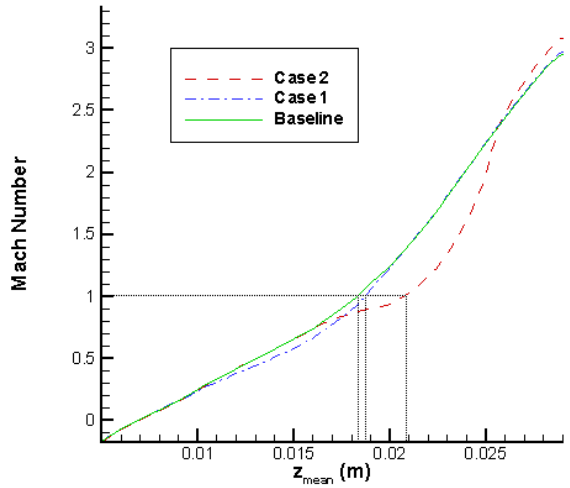

Figure 11: Time-Averaged Axial Profile of Mach Number. The sonic transition point is moved more toward the cathode for both case 1 and 2 compared to the baseline case. It is furthest toward the cathode in case 2. These cases correspond to those marked on figures 3 through 5.

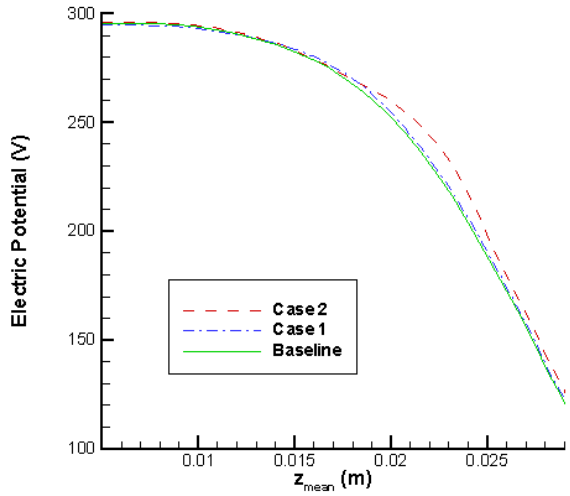

Figure 12: Time-Averaged Axial Profile of Electric Potential. In cases 1 and 2, the potential drop is modified in the region of the inserted insulator section with lower SEE coefficient. These cases correspond to those marked on figures 3 through 5.

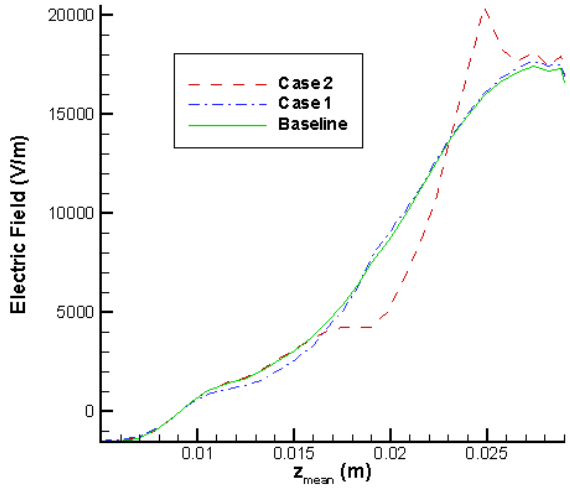

Figure 13: Time-Averaged Profile of Axial Electric Field. In cases 1 and 2, the electric field is localized in the region of the inserted insulator section with lower SEE coefficient. These cases correspond to those marked on figures 3 through 5.

Summary

Results from an evolved 2-D numerical Hall thruster simulation, HPHall, were compared to investigate the use of a section of channel insulator material with lower secondary electron emission (SEE) coefficient to increase thruster performance or reduce channel wall erosion. A channel insulator material similar to BN was used as a baseline with inserted sections of BNAlN ceramic. By varying the location and width of this insulator section, we found two operating regimes of interest.

A regime of increased performance was obtained when the section was placed mostly forward of the ionization zone. This performance increase is believed to be due to the increased electron temperature in the region where the SEE coefficient was reduced. It was also accompanied by an increase in ion flux to the walls. The increased ion wall flux is believed to result from localizing the electric field in the region of defocusing magnetic field lines, where the section with reduced SEE coefficient was placed. This problem may be counteracted with the use of sputter resistant materials near the thruster exit or by implementing a focusing magnetic field in the region of the inserted section.

A regime of reduced ion flux to the walls was obtained when the section was placed in the ionization zone. In this regime, the thrust and efficiency were be maintained or slightly increased from that of a continuous insulator. The reduced ion wall flux is believed to be due to the increased electric field in the region of focusing magnetic field lines. The ability of a section with lower SEE coefficient to localize the electric field in the region of focusing magnetic field lines appears to be limited due to the dominance of ionization losses over wall losses in this region.

We have shown that we might be able to modify the local plasma properties with the passive technique of replacing part of the channel insulator with a different ceramic material. We are still numerically investigating other ways this technique might be used and it should also be investigated experimentally. Future research should include an analysis of the effect of insulator discontinuities on the oscillatory characteristics of the discharge.

References

[1] S. Locke, U. Shumlak and J. M. Fife, "Effect of a Channel Wall Discontinuity in an SPT-Type Hall Thruster," *37th AIAA/ASME/SAE/ASEE Joint Propulsion Conference Proceedings*, July 8-11, 2001, AIAA-01-3327.

[2] A. Fruchtman, N. J. Fisch, "Modeling the Hall Thruster," 34th AIAA/ASME/SAE/ASEE Joint Propulsion Conference, Cleveland, OH, July 1998, AIAA-98-3500.

[3] Y. Raitses, D. Staack, A. Smirnov, A. A. Litvak, L. A. Dorf, T. Graves and N. J. Fisch, "Studies of Non-Conventional Configuration Closed Electron Drift Thrusters," *37th AIAA/ASME/SAE/ASEE Joint Propulsion Conference Proceedings*, July 8-11, 2001, AIAA-01-3776.

[4] Y. Raitses, L. A. Dorf, A. A. Litvak and N. J. Fisch, "Parametric Investigations of Segmented Electrode Hall Thruster," IEPC-99-245.

[5] J.M. Fife and S. Locke, "Influence of Channel Insulator Material on Hall Thruster Discharges: A Numerical Study," *39th AIAA Aerospace Sciences Meeting and Exhibit*, January 2001, AIAA-2001-1137.

[6] J. M. Fife, "Hybrid-PIC Modeling and Electrostatic Probe Survey of Hall Thrusters," PHD Thesis, Massachusetts Institute of Technology, September 1998.

[7] Mitchner and Kruger, *Partially Ionized Gases*, John Wiley & Sons, New York, 1973.

[8] J. R. M. Vaughan, A New for Secondary Emission Yield, *IEEE Transactions on Electron Devices*, Vol. 36, No 9, 1989, p 1963.

[9] L. Jolivet and J.-F. Roussel, "Effects of the Secondary Electron Emission of the Sheath Phenomena in a Hall Thruster," Space Propulsion Conference, Cannes, FR, October 2000.

[10] A. M. Bishaev and V. Kim, "Local Plasma Properties in a Hall-Current Accelerator with an Extended Acceleration Zone," Soviet Physics Technical Physics, 23(9):1055-1057, 1978.